

## Altered Sr environment in $\text{La}_{2-x}\text{Sr}_x\text{CuO}_4$

D. Haskel and E. A. Stern

*Department of Physics, Box 351560, University of Washington, Seattle, Washington 98195*

D. G. Hinks, A. W. Mitchell, and J. D. Jorgensen

*Materials Science Division, Argonne National Laboratory, Argonne, Illinois 60439*

(Received 22 April 1997)

The atomic arrangement about the Sr atoms in  $\text{La}_{2-x}\text{Sr}_x\text{CuO}_4$  was investigated by Sr *K*-edge polarized x-ray-absorption fine structure on oriented powder with  $x=0.075$  and  $0.1$  at  $T=20$  K. Our results confirm that Sr resides at the La lattice site but we discovered it induces major structural distortions in neighboring oxygen atoms. In particular, our best fits indicate that the O(2) apical oxygen to Sr is split into two sites separated by  $0.30(4)$  Å, providing evidence for a strong lattice-hole interaction, i.e., a polaron, which may be involved in the pairing mechanism of these cuprates. [S0163-1829(97)51026-5]

The mechanism by which Sr doping induces superconductivity in  $\text{La}_{2-x}\text{Sr}_x\text{CuO}_4$  is not fully understood. One of the questions yet to be answered experimentally is what is the effect of Sr substitution on the structure of its immediate atomic environment. The importance of this question is enormous. Chen *et al.*<sup>1</sup> found that doped holes in  $\text{La}_{2-x}\text{Sr}_x\text{CuO}_4$  have a significant amount of O  $2p_z$  orbital character, most likely associated with the O(2) apical oxygens, contrary to previous results ascribing a predominantly in-plane O  $2p_{x,y}$  and Cu  $3d_{x^2-y^2}$  orbital character to the doped holes. The relative importance of these out-of-plane orbitals *increases* with Sr content in the superconducting region of the phase diagram, and hence they could play a vital role in the charge-transfer mechanism leading to superconductivity in these cuprates. Knowledge of the local structure about the Sr atoms, in particular of their O(2) apical oxygens, is essential to fully understand these findings.

Experimental work using techniques sensitive to short-range order in the atomic arrangement has suggested the presence of Sr-induced atomic distortions. Sr *K*-edge x-ray-absorption near-edge structure (XANES) data<sup>2</sup> were interpreted to conclude that the introduction of Sr under normal preparation conditions leads to the removal of the O(2) apical oxygen to the Sr and the creation of an oxygen defect in a nearby interstitial site. Recent XANES theoretical calculations,<sup>3</sup> however, showed that the XANES features attributed by Tan *et al.*<sup>2</sup> to the removal of the apical oxygen to the Sr can be reproduced with the same oxygen configuration as about the La atoms. This controversy exemplifies the need of a quantitative determination of Sr-induced structural distortions in  $\text{La}_{2-x}\text{Sr}_x\text{CuO}_4$ .

A step in that direction was recently achieved when strong x-ray diffuse scattered intensity was observed in  $c^*$  cuts of reciprocal space in the neighborhood of Bragg peaks,<sup>4,5</sup> the momentum transfer dependence of the measured intensity implying distortions with a remarkable  $c$ -axis rms displacement  $\langle u_z^2 \rangle^{1/2} \approx 0.4$  Å. However, a more detailed knowledge of the Sr-induced atomic displacements is necessary if the effect of these distortions on the electronic structure of the doped material is to be quantitatively addressed.

Sr-induced distortions could also play a role in the mechanism of the low-temperature orthorhombic (LTO) to high-temperature tetragonal (HTT) dopant-induced structural phase transition. Contrary to the purely displacive character found by diffraction techniques,<sup>6</sup> pair distribution function analysis of neutron-scattering data<sup>7</sup> and x-ray-absorption fine structure (XAFS) (Ref. 8) show a significant order-disorder component for the transition, with the  $\text{CuO}_6$  octahedra remaining tilted as in the LTO phase (see Fig. 1) but becoming disordered relative to each other resulting in the HTT long-range order measured by diffraction. An increasing number of distorted domains introduced with Sr doping could be the disordering media.

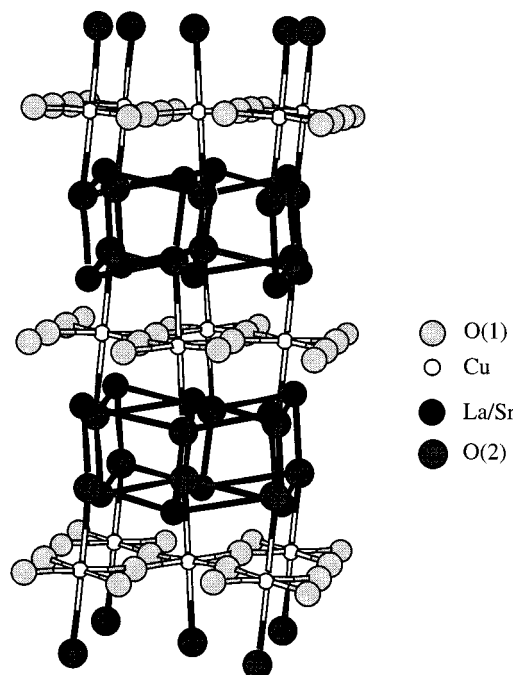


FIG. 1. Schematic representation of the  $\text{La}_{2-x}\text{Sr}_x\text{CuO}_4$  structure for  $x=0.075, 0.1$  at  $T=20$  K as found by neutron diffraction (Ref. 6).

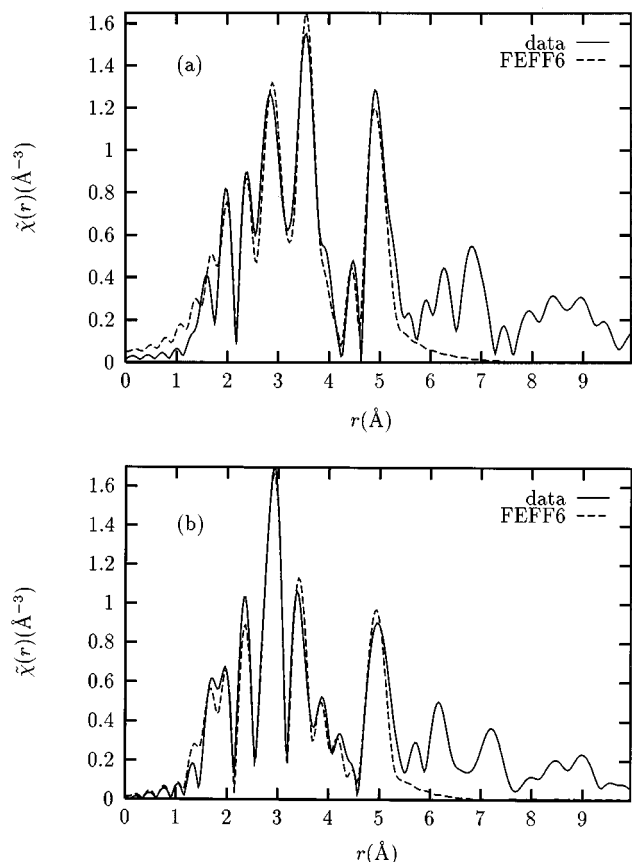


FIG. 2. Fits to the  $x=0.1$  sample at  $T=20$  K for x rays polarized (a) along the  $c$  axis and (b) in the  $ab$  plane. The magnitude of the complex Fourier transform of  $k^2\chi(k)$  is shown.

A number of unique features of XAFS spectroscopy were exploited in the present work to solve the question at hand. First, the Sr and La atomic environments were studied *separately* and directly compared, by tuning the x-ray energy to match the corresponding inner-shell electron excitation of either species. This is a key feature since the Sr and La atoms reside at the same crystallographic site and therefore diffraction techniques measure a Sr contribution which is only a few percent of the total signal at the Sr/La site.

Second, the orientation dependence of the XAFS signal was exploited by rotating the  $c$ -axis magnetically aligned-powder relative to the linearly polarized electric-field vector of the synchrotron radiation. Because of the anisotropy in the structure of  $\text{La}_{2-x}\text{Sr}_x\text{CuO}_4$ , polarized measurements allow for selectively probing different subsets of atoms (see Figs. 1 and 2). This is of importance to insure that the number of refinement parameters in the fit be less than the information content of the data.<sup>9</sup>

Finally, we exploited the high sensitivity of nearly collinear multiple-scattering (MS) paths to the presence of the intervening focusing atom<sup>10</sup> to determine the occupancy of the O(2) apical oxygen to the Sr atoms (see Fig. 3), even though its distance was highly disordered.

Samples used in this study are from the same batch used in the neutron-diffraction study of Radaelli *et al.*<sup>6</sup> and a detailed description of the sample preparation, superconducting properties, and their characterization as single phase can be found there. The sintered pellets were ground in a pestle and

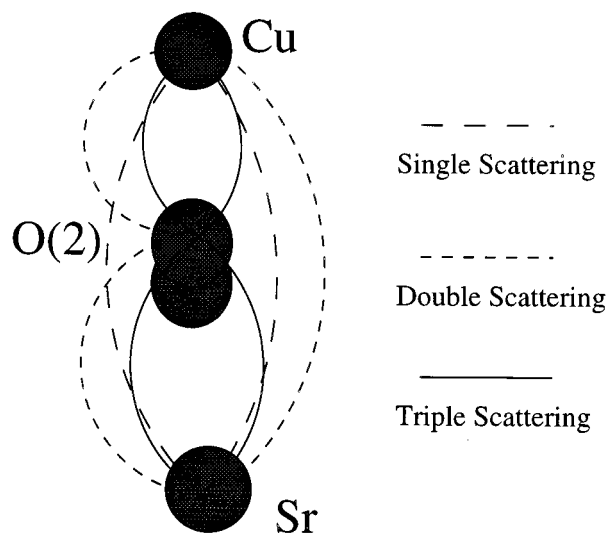


FIG. 3. Schematic representation of the SS and MS paths used to accurately determine the occupancy of the O(2) apical oxygen. The actual path deviates from collinearity by about  $8^\circ$ .

the resulting powder sieved to a typical  $20 \mu\text{m}$  grain size. The samples were oriented by a method described previously<sup>11</sup> and the high degree of  $c$ -axis orientation was confirmed by x-ray diffraction to be better than 95%; within the  $ab$  plane the orientation is random.

Sr  $K$ -edge measurements were performed in transmission at beamline X-11A of the National Synchrotron Light Source, using a Si(111) double-crystal monochromator. The harmonic content of the beam was minimized by detuning the second crystal. For the low-temperature measurements the samples were put in a sealed copper cell with Kapton windows, filled with He gas for thermal contact, and attached to a duplex refrigerator cold finger.

For powder oriented only in the  $c$  direction, the following holds for the XAFS of a single scattering (SS) path  $i$  at an angle  $\theta_i$  with the  $c$  axis:

$$\chi_c^{(i)}(k) = 3 \cos^2 \theta_i \chi_{ran}^{(i)}(k), \quad (1)$$

$$\chi_{ab}^{(i)}(k) = 3 \frac{\sin^2 \theta_i}{2} \chi_{ran}^{(i)}(k),$$

with  $\chi_c(k)$ ,  $\chi_{ab}(k)$  being the measured XAFS with the electric field parallel to the  $c$  and  $ab$  orientations, respectively, and  $\chi_{ran}(k)$  the XAFS signal of a completely unoriented powder.  $k$  is the photoelectron wave number.

We used FEFF6 code<sup>12</sup> as our theoretical standard to calculate the random XAFS  $\chi_{ran}(k)$  using the average atomic positions obtained in the diffraction studies and the UWXAFS analysis package<sup>13</sup> to *simultaneously* fit both polarized XAFS data to the theory by weighting their respective amplitudes as given in Eq. (1) and varying  $\theta_i$ . In addition, adjustable structural parameters were added to the theory, such as changes in half path length,  $\delta r_i$  and mean-square displacements,  $\sigma_i^2$ , to account for possible deviations in the local structure from the average structure. Simultaneous fits to both polarizations allow a reduction in the number of fitting parameters for scattering paths which contribute to both

$c$  and  $ab$  oriented XAFS. This procedure was initially applied to fit the data up to  $r \approx 4 \text{ \AA}$  where only O, Cu, and La/Sr single-scattering paths contribute to the XAFS (see Fig. 1).

The fitting of the theory to the data is done in  $r$  space and the uncertainties determined from a reduced  $\chi^2_\nu$  using standard techniques of error analysis.<sup>13,14</sup> Data and theory in a  $k$ -range (3,14)  $\text{\AA}^{-1}$  were weighted by  $k^2$  and Fourier transformed to  $r$  space. The region of  $r$  space fitted was expanded to  $r = (1.9, 5.3) \text{ \AA}$  and included required MS paths. The total number of independent points is  $N_I = 48$  while the number of fitting parameters used is  $N_p = 26$ .

Figure 2 shows best fits to both orientations for the  $x = 0.1$  sample at  $T = 20 \text{ K}$ . Typically, the noise in the data is about three times smaller than the difference between the fit and data averaged over our fitting range, indicating systematic errors dominate in the uncertainties of the parameters.

Our main results can be summarized as follows.

(a) The Sr-Cu and Sr-La distances and mean-square displacements up to the fifth shell are, within  $0.01 \text{ \AA}$  and  $0.001 \text{ \AA}^2$ , respectively, the same as those as for La-Cu and La-La found in the fittings to La  $K$ -edge polarized data<sup>8</sup> and in agreement with the distances found by diffraction for the average structure. This result confirms that Sr indeed substitutes at the La site and is consistent with the  $\text{Sr}^{2+}$  and  $\text{La}^{3+}$  ions having nearly the same size. The fact that the Sr's are not themselves displaced from the average lattice positions is in agreement with the observation of no change in diffuse scattering when scanning the x-ray energy through the Sr  $K$ -edge resonance.<sup>4</sup> The Cu atoms being at the average lattice positions rules out the possibility of neighboring Cu atoms to Sr contributing to the observed diffuse scattering.

(b) Since the Sr-O(2) apical SS signal at  $r \approx 2.35 \text{ \AA}$  is small, it was not possible to unambiguously separate the effect of O(2) occupancy from that of disorder on the amplitude of the SS path. On the other hand, the nearly collinear focusing MS paths Sr-O(2)-Cu at  $r \approx 4.76 \text{ \AA}$  (Fig. 3) are insensitive to the disorder of the focusing atom but their phase and amplitude are extremely sensitive to the presence of the intervening O(2) focusing atom.<sup>10</sup> Hence we *simultaneously* fitted the Sr-O(2) SS path and the Sr-O(2)-Cu MS paths to self-consistently and accurately determine the O(2) apical occupancy, position, and disorder.

We found that the O(2) apical oxygen to the Sr atom is fully occupied, its value being  $N = 0.92 \pm 0.2$ . Initially a Gaussian disorder was assumed and found for the Sr-O(2) apical bond to be  $\sigma^2 = 0.026 \pm 0.01 \text{ \AA}^2$ , compared to a  $\sigma^2 = 0.002(1) \text{ \AA}^2$  for La-O(2) apical. A Sr-O(2) distance  $r = 2.49 \pm 0.1 \text{ \AA}$  was obtained instead of the  $2.35 \text{ \AA}$  found for La-O(2) apical<sup>8</sup> and in the diffraction studies.<sup>6</sup> The large uncertainties arise because a Gaussian disorder is a bad model for the Sr-O(2) apical bond, as discussed below. The  $\delta r$  and  $\sigma^2$  obtained for the Sr-O(2)-Cu MS paths, however, are within  $0.01 \text{ \AA}$  and  $0.001 \text{ \AA}^2$ , respectively, the same as for the La central atoms and in agreement with the average structure, indicating that the displacement of the O(2) apical oxygen is along the  $c$  axis and hence does not affect the total path length of the MS paths (Fig. 3).

A striking feature is the order of magnitude greater disorder of the O(2) atom compared to that of the surrounding Cu and Sr atoms in Fig. 3. This is quite unusual since for a

constant potential between O(2) and its neighbors one would expect a fluctuating force from the large  $\sigma^2$  which would increase the  $\sigma^2$  between the Sr and Cu atoms. A possible explanation is that the potential sensed by the O(2) atom is not constant but is fluctuating depending on the number of hole carriers at the Cu site. This fluctuation causes the O(2) to fluctuate between two sites, both of which are in equilibrium as in the model of a negative  $U$  center<sup>15</sup> or ‘‘anti-Jahn-Teller’’ polaron<sup>16</sup> and thus does not displace the Cu and Sr atoms. This strong lattice-hole interaction could be involved in the pairing mechanism.

To test this assumption we isolated the O(2) apical signal by subtracting from the data (in  $r$  space) the contribution of all other paths as obtained in the best fit and back Fourier transforming to  $k$  space. A comparison of the fitted O(2) apical contribution to the isolated signal showed that a single distance and a  $\sigma^2$  were not enough to fit the O(2) apical XAFS. By fitting the isolated signal with a two-shell model, however, a more than a factor of 2 improvement in reduced  $\chi^2_\nu$  was obtained, even though the normalization divider  $\nu$ , the degrees of freedom, was reduced by two additional parameters (a splitting and the relative occupancy of the two sites). The best fit gives equal occupancy for both sites,  $\sigma^2 = 0.002(1) \text{ \AA}^2$ ,  $r_1 = 2.55(2) \text{ \AA}$ ,  $r_2 = 2.25(3) \text{ \AA}$ . The center of the distribution is displaced from the neutron-diffraction value by  $\delta r = 0.05(4) \text{ \AA}$  toward the Cu atoms and the separation between sites is  $\Delta = 0.30(4) \text{ \AA}$ .

To further test this model we studied the temperature dependence of the  $x = 0.1$  sample at  $T = 120 \text{ K}$ , and  $300 \text{ K}$ . Whereas the mean-square disorder in all other distances can be described by harmonic Einstein oscillators, the big  $\sigma^2$  of the Sr-O(2) bond obtained with a single-shell model doesn't show any appreciable  $T$  dependence. A harmonic potential would have led, at  $300 \text{ K}$ , to a  $\sigma^2 \sim$  ten times larger than our measured value. This is inconsistent with a single-site, harmonic potential for the O(2) but consistent with the two-site model whose overall disorder arises predominantly from the temperature independent splitting of the two sites.

We note that whereas a split apical oxygen site has been observed in several high- $T_c$  compounds,<sup>17</sup> the discovery of such lattice anomaly *only* at a dopant site is different [we found no evidence for a double site O(2) configuration about the La atoms]. Our result indicates that hole doping induced by Sr coexists with local lattice distortions, which could define a more active role for Sr in the mechanism of high- $T_c$  superconductivity.

The implications of the distortion in the O(2) apical oxygen distance are many. The O(2) site closer to the Cu-O planes couples more effectively to them and explains the increase with Sr concentration of out-of-plane O  $2p_z$  character of the doped holes observed by Chen *et al.*<sup>1</sup> Also, the fluctuating O(2) apical atoms provide a more effective ‘‘bridge’’ between the Cu-O and La-O layers and hence explain the relative increase in out-of-plane conductivity with doping.<sup>18</sup> Adding the effective  $c$ -axis static displacement of  $0.05 \text{ \AA}$  to the effective rms displacement  $(\Delta/2) = 0.15 \text{ \AA}$  we get an rms deviation from the average structure  $\langle u_z^2 \rangle^{1/2} \approx 0.16 \text{ \AA}$ . This is a significant contribution to the measured rms displacement of the atoms contributing to the diffuse scattering.<sup>4</sup>

(c) The average structure has two different La/Sr-O(1) distances to the O(1) oxygens in the Cu-O planes at  $r_s=2.591$  Å and  $r_l=2.675$  Å. La-O(1) distances were found by XAFS to be in agreement with the diffraction results.<sup>8</sup> The splitting is mainly due to the tilt pattern of the CuO<sub>6</sub> octahedra which buckles the Cu-O planes<sup>6</sup> (see Fig. 1). In the Sr XAFS analysis, we find the angles these bonds form with the *c* axis to be  $\theta^{(s)}=44.1\pm 6.1^\circ$  and  $\theta^{(l)}=41.9\pm 6.2^\circ$ , respectively, consistent with the values  $\theta^{(s,l)}=47.8^\circ, 44.2^\circ$  found in the diffraction studies.<sup>6</sup> However, the Sr-O(1) distances are found to be  $r_s=2.542(10)$  Å and  $r_l=2.734(12)$  Å, respectively.

In order to accommodate the changes in Sr-O(1) distances while the Sr-Cu distances remain unaltered, the Cu-O(1) bonds in the basal plane of the CuO<sub>6</sub> octahedra involving these O(1) oxygens must become distorted compared to the average structure. These distortions are *not* associated with a *rigid* tilt of the CuO<sub>6</sub> octahedra involved since that would have caused a related distortion of the O(2) oxygens forming the apex of the CuO<sub>6</sub> octahedra and nearly coplanar with the Sr, which is not the case (Fig. 4). Thus the observed distortions perturb the periodicity in the arrangement of the CuO<sub>6</sub> octahedra.

(d) Concomitant with the *c*-axis distortion of the O(2) apical oxygen described in (b), we found correlated displacements of neighboring, nearly coplanar O(2) and La atoms. Figure 4 summarizes the pattern of displacements induced by the presence of the Sr. The O(2) oxygens at distances  $r=4.37$  Å and  $r=4.53$  Å from the Sr atoms, are displaced by  $0.14\pm 0.02$  Å and  $0.11\pm 0.03$  Å from their average positions, respectively, towards the distorted O(2) apical. The La atoms at  $r=3.95$  Å are slightly displaced inwards by  $0.03\pm 0.01$  Å and those at  $3.97$  Å are displaced outwards by  $0.023\pm 0.01$  Å.

To summarize, when Sr substitutes for La in La<sub>2-x</sub>Sr<sub>x</sub>CuO<sub>4</sub> it does more than just donate a hole. It resides at the La lattice site but distorts considerably its near-neighbor oxygen environment. In particular, the two-site O(2) apical distortion found in our best fits is quantitatively important for the hole doping mechanism in these cuprates,

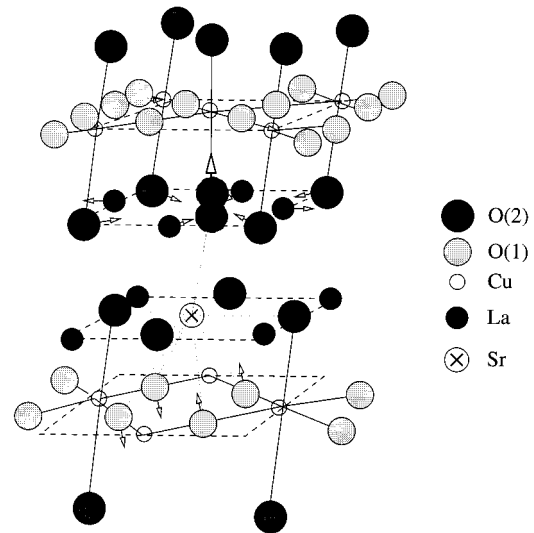


FIG. 4. Schematic representation of the pattern of atomic displacements induced by Sr substitution, as measured by XAFS.

their transport properties, and correlates a strong lattice distortion to the hole donated by the Sr atoms, i.e., a polaron. To prove that this polaron is related to the pairing mechanism will require further investigation. The Sr substitution disorders the neighboring CuO<sub>6</sub> octahedra from their periodic structure. This could be an important factor in understanding the mechanism of the Sr-induced structural phase transitions in this material. Finally, the Sr-induced distortions are the origin of the observed diffuse scattering in these cuprates.

The valuable help of F. Perez and M. Suenaga in orienting the samples is greatly appreciated, as well as helpful discussions with J. Budnick, A. Frenkel, B. Ravel, G. Seidler, and Y. Yacoby. The work at the University of Washington was done under the auspices of DOE Grant No. DE FG06-90ER45425. The work at Argonne National Laboratory was supported by DOE Contract No. W-31-109-ENG-38 and NSF Grant No. DMR 91-20000.

<sup>1</sup>C. T. Chen *et al.*, Phys. Rev. Lett. **68**, 2543 (1992).

<sup>2</sup>Z. Tan *et al.*, Phys. Rev. Lett. **64**, 2715 (1990).

<sup>3</sup>Z. Y. Wu *et al.*, Physica B **208&209**, 491 (1995).

<sup>4</sup>E. D. Isaacs *et al.*, Phys. Rev. Lett. **72**, 3421 (1994).

<sup>5</sup>W. Dmowski *et al.*, Phys. Rev. B **52**, 6829 (1995).

<sup>6</sup>P. G. Radaelli *et al.*, Phys. Rev. B **49**, 4163 (1994).

<sup>7</sup>T. Egami *et al.*, Rev. Solid State Sci. **1**, 247 (1987).

<sup>8</sup>D. Haskel *et al.*, Phys. Rev. Lett. **76**, 439 (1996).

<sup>9</sup>E. A. Stern, Phys. Rev. B **48**, 9825 (1993).

<sup>10</sup>P. A. Lee and J. B. Pendry, Phys. Rev. B **11**, 2795 (1975).

<sup>11</sup>S. M. Heald *et al.*, Phys. Rev. B **38**, 761 (1988).

<sup>12</sup>S. Zabinsky *et al.*, Phys. Rev. B **52**, 2995 (1995).

<sup>13</sup>E. A. Stern *et al.*, Physica B **208&209**, 117 (1995).

<sup>14</sup>M. Newville *et al.*, Physica B **208&209**, 154 (1995).

<sup>15</sup>Y. Bar-Yam, Phys. Rev. B **43**, 359 (1991); Phys. Rev. B **43**, 2601 (1991).

<sup>16</sup>V. I. Anisimov *et al.*, Phys. Rev. Lett. **68**, 345 (1992); H. Kamimura, Jpn. J. Appl. Phys. 2, Lett. **26**, L627 (1987).

<sup>17</sup>S. D. Conradson, Science **248**, 1394 (1990); J. Mustre de Leon *et al.*, Phys. Rev. Lett. **65**, 1675 (1990); T. Egami *et al.*, Physica C **185-189**, 867 (1991).

<sup>18</sup>S. Kambe *et al.*, Physica C **160**, 35 (1989).